AMMONIA MEASUREMENTS BY THE NASA TROPOSPHERIC EMISSION SPECTROMETER (TES)

Karen E. Cady-Pereira*
Atmospheric and Environmental Research, Lexington, MA, USA

M. W. Shephard
Environment Canada, Toronto, ON, CANADA

D. K. Henze and L. Zhu
University of Colorado, Boulder, CO, USA

R. W. Pinder, J. O. Bash and J. T. Walker
U.S. Environmental Protection Agency, Research Triangle Park, NC, USA

M. Luo
Jet Propulsion Laboratory, Pasadena, CA, USA

1. INTRODUCTION

Ammonia (NH_3) is a highly reactive gas emitted principally by animal waste and fertilizer application, and to a lesser extent by industrial activity, mining and automobiles. Ammonia contributes significantly to several well-known environmental problems; excess deposition in terrestrial ecosystems can lead to soil acidification and loss of plant diversity; in coastal ecosystems, it can cause eutrophication, algal blooms, and loss of fish and shellfish. In the atmosphere NH_3 can combine with sulfates and nitric acid to form ammonium nitrate and ammonium sulfate, which constitute a substantial fraction of fine particulate matter (PM2.5). These particles are statistically associated with health impacts (Pope et al., 2000) and contribute to radiative forcing by the atmosphere, while also impacting visibility. Morever, the in situ measurements that are available show high levels of spatial and temporal variability (Carmichael et al., 2003; Walker et al., 2004). Nevertheless the knowledge of the magnitude and seasonal/spatial variability of the emissions is severely limited, and this limitation impacts the capability of models to predict ammonia concentrations.

Beyond estimating the current impact of NH_3 on air quality, correct emissions are important for predicting the trend in NH_3 concentrations. It is estimated that 80% of the ammonia emitted into the atmosphere has agricultural sources. The rapid increase in fertilizer use (Erisman et al., 2008), especially in developing countries such as India and China, is expected to lead to ever greater amounts of NH_3 in the atmosphere, further disrupting the nitrogen cycle. In addition, since sulfate and nitrate concentration are decreasing due to government regulations, NH_3 will become the dominant player in PM2.5 formation. In summary, far more data on current NH_3 distribution and variability are required than are currently available.

*Corresponding author: Karen Cady-Pereira, Atmospheric and Environmental Research, 131 Hartwell Ave, Lexington, MA, 02421-3126; e-mail: kcadyper@aer.com

2. CHARACTERISTICS OF TES AMMONIA MEASUREMENTS

2.1 Ammonia from space

Satellite observations of tropospheric ammonia can provide an estimate of the current NH_3 distribution over the globe, including over regions with few or no in situ measurements. Moreover, they will also allow for an evaluation of the change in this distribution over time. The first satellite observations of boundary layer tropospheric ammonia were reported by Beer et al., (2008) using the Troposheric Emission Spectrometer (TES) nadir infrared FTS spectra. That study presented preliminary TES retrievals over a limited range of conditions. The Infrared Atmospheric Sounder Interferometer (IASI), an instrument similar to TES but with lower spectral resolution, also retrieves NH_3 in nadir viewing

mode using the thermal infrared spectral region. The excellent spatial coverage of the IASI instrument, coupled with a very simple and fast retrieval based on the conversion of brightness temperature differences into total column measurements, have provided a global picture of the distribution of ammonia (Clarisse et al., 2009). *Clarisse et al.,* (2010) using a more refined algorithm provided greater insight into the remote sensing of tropospheric ammonia presenting several sensitivity issues, principally the impact of the thermal contrast on the boundary layer retrievals of ammonia.

TES has less dense spatial coverage than scanning satellites (e.g. IASI, AIRS), but has a higher spectral resolution of 0.06 cm-1 (compared to more typical scanning infrared satellite sensors with 0.5-1.0 cm-1). The combination of the higher spectral resolution and good signal-to-noise (SNR) of the TES instrument in the ammonia region (Shephard et al., 2008) provides increased sensitivity to ammonia concentrations near the surface from satellite observations. In addition, TES is in a sun-synchronous orbit that has a local overpass time of 1330 mean solar time, providing favorable conditions for increased thermal contrast and thus increased sensitivity to boundary layer ammonia (Clarisse et al., 2010). The high spectral resolution also allows for selection of spectral regions (microwindows) that reduce the impact of interfering species, and therefore, systematic errors in the retrievals. These TES sensor characteristics and a sophisticated global retrieval algorithm provide a capability to globally monitor ammonia. In spite of the reduced coverage the global maps created from TES NH_3 (Shephard et al., 2011) show some of the same features present in the IASI maps (Clarisse et al., 2009), most notably the hotspot over the Indian subcontinent.

2.2 TES Ammonia

Ammonia is spectrally active across the 800-1200 cm-1 range, which contains the NH_3 ν_2 vibrational band, but has its strongest feature in the Q-branch around 967 cm-1 (Figure 1). The TES NH_3 retrieval algorithm uses the radiances in microwindows across this feature to obtain profiles of NH_3. The TES NH_3 averaging kernel, (see example in the left panel of Figure 2), which represents the sensitivity of the retrieved value at one level to the true value at every level, has peak sensitivity between 900 and 700 mbar and a degrees of freedom for signal (DOFS) on the order of 1 or less. The DOFS is correlated with the information content of the TES NH_3 signal; a value of 1 signifies that there is only one piece of information, and that the profile shape will be strongly influenced by the selected a priori profile. However, one can collapse the available information to a single value, the Representative Volume Mixing Ratio (RVMR), through a mapping based on the TES sensitivity (right panel of Figure 2). The RVMR is much less influenced by the a priori choice (Shephard et al., 2011) and provides a useful metric for comparisons with point surface or aircraft measurements.

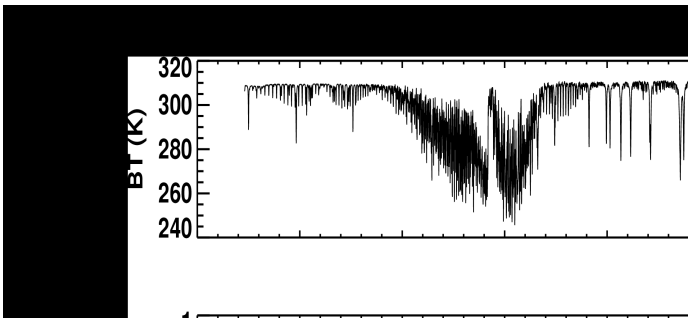

Figure 1: Simulated TES spectrum (top) and NH_3 signal (bottom)

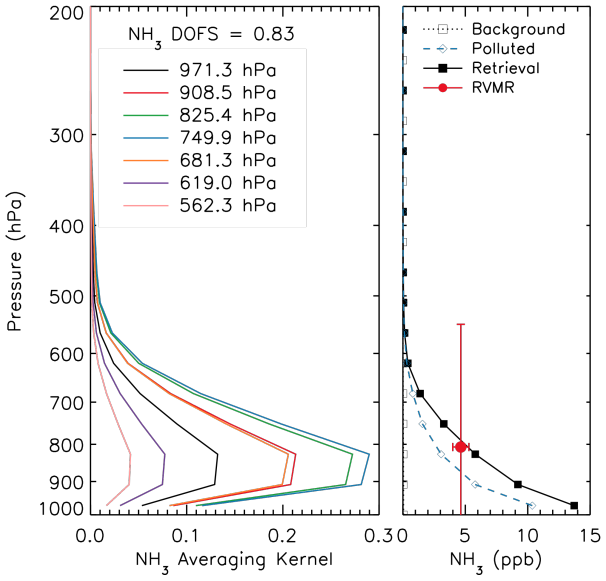

Figure 2: Sample TES NH_3 averaging kernel (left); a priori and retrieved profiles and retrieved RVMR (right). The red bar represents the region over which the RVMR is representative.

An important criteria for users of TES NH_3 data is detectability. For ammonia detectability is driven principally by the concentration and by the thermal contrast, the differences between the surface temperature and the temperature of the layer just above the surface, where most atmospheric NH_3 is found. We used simulated TES radiances from a set of profiles from around the globe and spanning a range of ammonia values to estimate the Signal to Noise Ratio (SNR) in the TES NH_3 retrieval microwindow. We found that TES requires a minimum of 1 ppbv with good thermal contrast, and that detectability decreases with decreasing thermal contrast. (Shephard et al., 2011).

3. EVALUATING SINGLE TES MEASUREMENTS

Evaluating the accuracy of TES NH_3 is not a trivial procedure. The TES RVMR is a metric determined by the amount and distribution of NH_3 in a column with a 5.3x8.3 km footprint, while aircraft and surface network NH_3 values are point measurements. Given the inherent spatial and temporal variability in NH_3 concentrations, absolute comparisons are difficult. Surface measurements have the additional complication of frequently being averages over time. Here we present data taken in the San Joaquin Valley in California, where the combination of intensive agriculture, leading to high NH_3 concentrations (as high as 1000 ppbv), and strong thermal contrast, provides an excellent site for evaluating the TES algorithm. Several aircraft campaigns have collected NH_3 in situ measurements collocated with TES, and the data have shown that TES NH_3 is well correlated with the in situ measurements.

We will compare TES transects, a series of closely spaced observations, with measurements from aircraft or surface vehicles moving along or close to the TES flight path. These data were obtained from the northern San Joaquin Valley, during the DISCOVER-AQ campaign in January 2013 and during the California Nexus (CalNex) spring 2010 campaign. The examples illustrate the TES performance under nearly ideal conditions: high NH3 concentrations, no clouds and good thermal contrast.

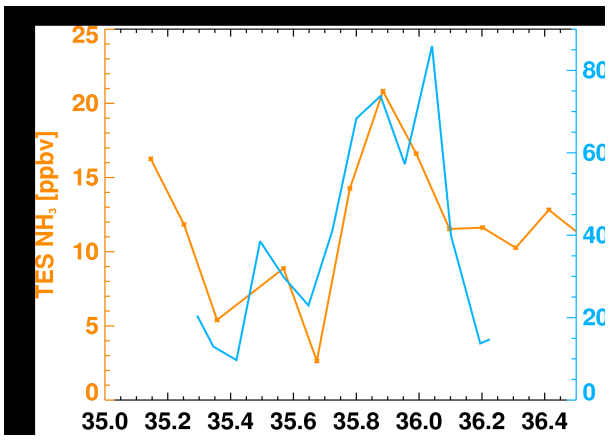

Figure 3: NH_3 on January 28 over the San Joaquin Valley, measured by TES (in gold) and by the Open Air QCL in blue.

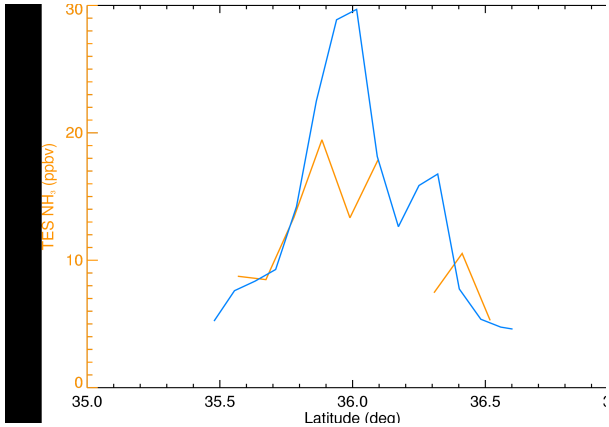

Figure 4: NH3 on January 21, 2013, over the San Joaquin Valley, measured by TES (in gold) and by the CIMS on the P3B aircraft (in blue). CIMS data have been averaged along the TES footprint.

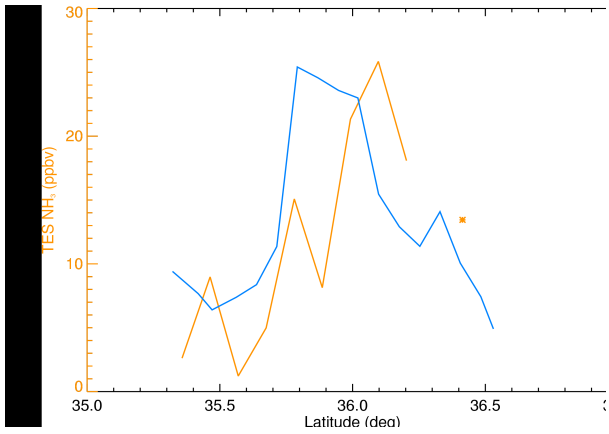

Figure 5: Same as Figure 5, but for data taken on January 30, 2013.

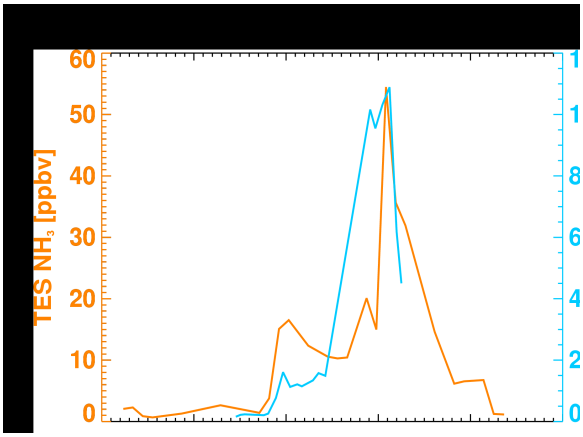

Figure 6: NH3 over the San Joaquin Valley, measured on May 14, 2010 by TES (in gold) and on May 12 by the CIMS on the P3B aircraft (in blue). CIMS data have been averaged along the TES footprint.

Figures 3 through 5 present data taken during DAQ-2013 in January, while Figure 6 shows data from May 2010. The in situ data from Figure 3 are from an Open QCL mounted on a vehicle closely following the TES track, while the in situ data for Figures 4 through 6 are from the CIMS instrument mounted on the P3B aircraft flying 300-500 m above the ground. The measurement times differ. While the TES data are always taken at approximately 1:15pm local solar time, the QCL data were collected over the 11:30 to 15:30 pm period, the aircraft data from DAQ were taken an an hour before the TES overpass, and the aircraft data from CalNex were taken around 5:30pm, two days before the TES transect. Given the range in sampling time and the footprint issues discussed above, the generally good spatial correlation between TES and the in situ measurements suggests that the spatial variability in NH_3 in the valley does not change substantially over short time scales, i.e, a strong source region tends to remain a strong source region, though the total emitted NH3 may vary, driven principally by temperature changes. The peak in concentration falls consistently around 36N, in an area near Tipton, where there are a large number of diary farms. However, the peak value is much higher in May, when the surface temperature is 299 K, as compared to 280 K in January. In summary, TES has the sensitivity to capture spatial and temporal variability of surface NH3 concentrations over a strong source region. Relating the TES measured values to the actual surface values is more difficult.

4. AVERAGING TES NH3

When NH_3 amounts are closer to the detection limit, or TES coverage is sparser, evaluating the TES data requires averaging over time and/or space. We analyzed datasets over two regions which included strong NH_3 sources, but with weaker thermal contrast and over a longer period, which lead to many observations below the TES detection limit.

In 2009 TES collected transect data over North Carolina from February through December. During the same period the EPA collected data from its Carolina Ammonia Monitoring Network (CAMNeT) consisting of ALPHA passive samplers, which provided two week means of NH_3 at the surface. A number of the samplers were placed directly under the TES track. However, the difficulty of relating two week means of point measurements to instantaneous TES samples with a large footprint once every two weeks precluded direct comparisons as done in section 3. Instead Pinder et al. (2011) calculated monthly averages of CAMNeT and TES daytime values. Nighttime values were excluded because they are not correlated with the two week means: weak vertical mixing at night leads to pooling of NH_3 near sources and much greater temporal and spatial variability. The monthly means from both TES and CAMNeT show a similar seasonal cycle, even though the TES data were fairly sparse due to frequent cloudy conditions.

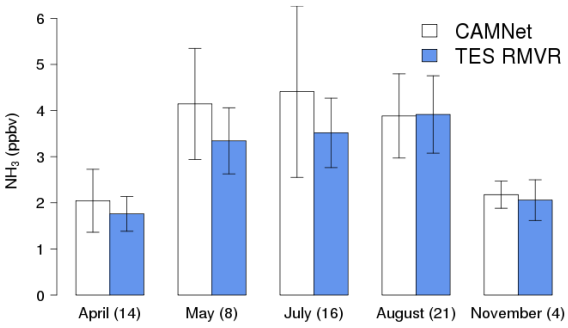

Figure 7: NH_3 monthly means from CAMNeT and TES over North Carolina in 2009

Pinder et al. (2011) also analyzed spatial variability by binning each TES and CAMNeT observation by the number of livestock facilities

within a 10 km radius of the observation (Figure 8). Once again the results from TES and CAMNeT are in agreement.

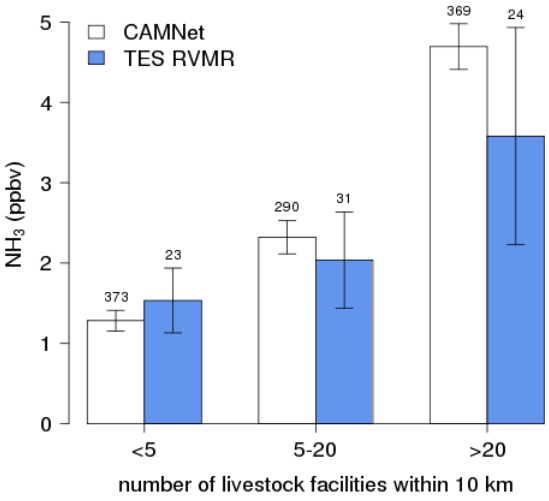

Figure 8: CAMNeT and TES NH3 binned by number of livestock facilities over North Carolina in 2009.

TES also collected a long series of transects over eastern China, passing over Beijing, from 2007 through 2009. Figure 9 shows the TES time series over Beijing, averaged by month, and a coincident set of monthly surface observations reported by Meng et al. (2011). The seasonal cycle recorded by TES correlates well with the surface measurement.

We have shown that under ideal conditions TES NH_3 is well correlated with surface measurements. Under more challenging conditions, e.g., smaller NH_3 concentrations, weaker thermal contrast or frequent cloudiness, the TES NH3 signal is weaker and it is not possible to make point by point comparisons. Nevertheless, by averaging this weak signal the uncertainties due to environmental factors are reduced and the resulting data shows the potential of TES to provide temporal and spatial variability.

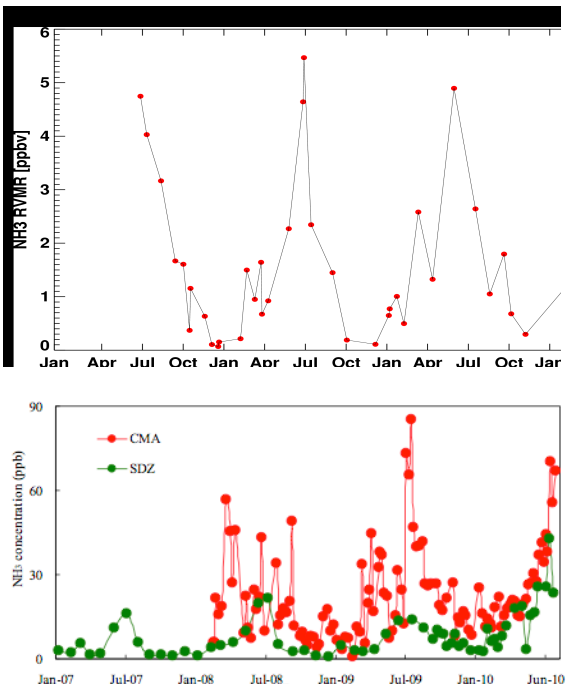

Figure 9: TES NH3 monhly means from 2007 through 2009 over Beijing (top) and surface measurements over the same period (from Meng et al., 2011).

5. USING TES NH_3 TO CONSTRAIN EMISSIONS IN A GEOCHEMICAL TRANSPORT MODEL

We have shown that TES measurements contain information regarding NH_3 concentrations. Zhu et al. (2013) have used the TES NH_3 retrieved profiles from April, July and October in the 2006-2009 period, along with the corresponding error estimates and averaging kernels, in an adjoint based inversion to constrain NH_3 emissions in the geochemical transport model GEOS-Chem over North America (Figure 10). The inversion suggested that significant changes were required over the western US and Mexico to match the TES observations.

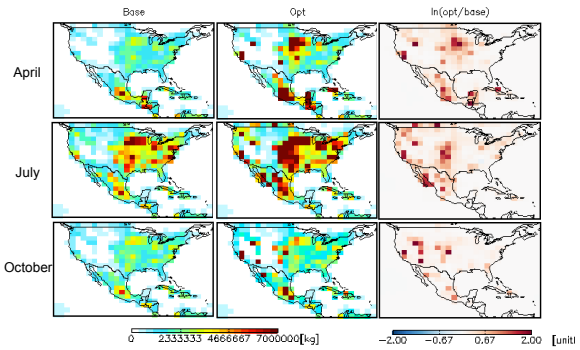

Figure 10: NH3 emissions from GEOS-Chem before and after the optimization.

GEOS-Chem was then run with these optimized emissions and the output was compared with in situ measurements from the AMoN network (Figure 11). The optimized model does a better job of capturing the range and variability of NH3 at the AMoN sites in April and October, but is biased high in July. The bias may be due to the 1 ppbv TES level of detectability, which leads to a sampling high bias. These results illustrate the potential of using TES NH3 to constrain emissions, but also point to the need for further work developing improved assimilation algorithms.

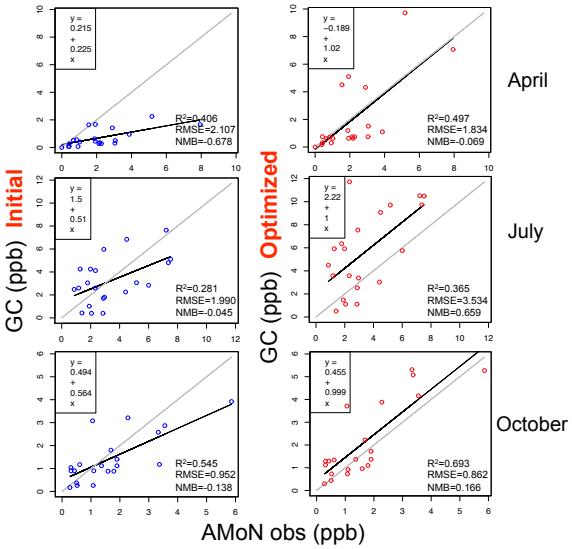

Figure 11: Comparison of GEOS-Chem NH3 concentrations with observations from AMoN sites before and after the optimization. The square of the correlation coefficient (R2), root mean square error (RMSE),and normalized mean bias (NMB) are shown. Black solid lines are regressions. Gray dashed lines are 1:1.

6. CONCLUSIONS

Under optimal observing conditions, over strong source regions and high thermal contrast, TES NH_3 observations correlate well with in situ measurements. In less ideal conditions, averages of TES data can still provide useful information on temporal and spatial variability, and can be used in inverse modeling to constrain emissions.

7. REFERENCES

Beer, R., M. W. Shephard, S. S. Kulawik, S. A. Clough, A. Eldering, K. W. Bowman, S. P. Sander, B. M. Fisher, V. H. Payne, M. Luo, G. B. Osterman, and J. R. Worden, 2008: First satellite observations of lower tropospheric ammonia and methanol. *Geophys. Res. Lett.,* **35**, L09801, doi:10.1029/2008GL033642.

Carmichael, G. R., and Coauthors, 2003: Measurements of sulfur dioxide, ozone and ammonia concentrations in Asia, Africa, and South America using passive samplers. *Atmos. Environ.,* **37**(9–10), 1293–1308, doi:10.1016/ S1352-2310(02)01009-9.

Clarisse, L., C. Clerbaux, F. Dentener, D. Hurtmans, and P.-F. Coheur, 2009: Global ammonia distribution derived from infrared satellite observations. *Nat. Geosci.,* **2**(7), 479–483.

Clarisse, L., M. W. Shephard, F. Dentener, D. Hurtmans, K. Cady-Pereira, F. Karagulian, M. Van Damme, C. Clerbaux, and P.-F. Coheur, 2010: Satellite monitoring of ammonia: A case study of the San Joaquin Valley. *J. Geophys. Res.*, **115**, D13302, doi:10.1029/2009JD013291.

Erisman, J. W., A. Bleeker, A. Hensen, and A. Vermeulen, 2008: Agricultural air quality in Europe and the future perspectives. *Atmos. Environ.,* **42**, 3209–3217.

Meng, Z. Y., W. L. Lin, X. M. Jiang, P. Yan, Y. Wang, Y. M. Zhang, X. F. Jia, and X. L. Yu, 2011: Characteristics of atmospheric ammonia over Beijing, China. *Atmos. Chem. Phys.*, **11**, 6139-6151, doi:10.5194/acp-11-6139-2011.

Pinder, R. W., J. T. Walker, J. O. Bash, K. E. Cady-Pereira, D. K. Henze, M. Luo, G. B. Osterman, and M. W. Shephard, 2011: Quantifying spatial and temporal variability in atmospheric ammonia with in situ and space-based observations. *Geophys. Res. Lett.*, **38**,

L04802, doi:10.1029/2010GL046146.

Pope, C. A., 2000: Epidemiology of fine particulate air pollution and human health: Biologic mechanisms and who's at risk? *Environ. Health Perspect.*, **108**, 713–723.

Shephard, M.W.,Worden, H. M., Cady-Pereira, K. E., Lampel, M.,Luo, M., Bowman, K. W., Sarkissian, E., Beer, R., Rider, D. M.,Tobin, D. C., Revercomb, H. E., Fisher, B. M., Tremblay, D.,Clough, S. A., Osterman, G. B., and Gunson, M., 2008: TroposphericEmission Spectrometer Spectral Radiance Comparisons, J. *Geophys.Res*., **113**, D15S05, doi:10.1029/2007JD008856

Shephard, M. W., Cady-Pereira, K. E., Luo, M., Henze, D. K., Pinder, R. W., Walker, J. T., Rinsland, C. P., Bash, J. O., Zhu, L., Payne, V. H., and Clarisse, L., 2011: TES ammonia retrieval strategy and global observations of the spatial and seasonal variability of ammonia, *Atmos. Chem. Phys*., **11**, 10743–10763, doi:10.5194/acp-11-10743-2011, 2011.

Walker, J. T., D. R. Whitall, W. Robarge, and H. W. Paerl, 2004: Ambient ammonia and ammonium aerosol across a region of variable ammonia emission density. *Atmos. Environ.,* **38**(9), 1235–1246, doi:10.1016/ j.atmosenv.2003.11.027.

Zhu, L., D. K. Henze, K. E. Cady-Pereira, M. W. Shephard, M. Luo, R. W. Pinder, J. O. Bash, and G.-R. Jeong, 2013: Constraining U.S. ammonia emissions using TES remote sensing observations and the GEOS-Chem adjoint mode. *J. Geophys. Res.*, **118**, doi:10.1002/jgrd.50166.